ANALYSIS OF PLATES ON ELASTIC FOUNDATION BY THE FINITE ELEMENTS METHOD

BARROS, J.A.O.
Assistent Prof.
University of Minho
Braga, Portugal

BARREIROS MARTINS, J.
Professor
University of Minho
Braga, Portugal

SUMMARY

The Mindlin's theory for the bending of plates is formulated by the finite elements method in order to the analysis of plate structures resting on elastic media. The foundation soil is represented by springs with linear elastic behaviour (Winkler's theory).

A programme has been developped for small computers. It consists of three moduli: preprocessing which includes data preparation with graphic treatment (network generation and renumbering, etc.); displacements and support reactions calculation for each loading system; postprocessing, including options with numerical files creation and graphical treatment of results.

The stiffness of the foundation soil can vary from point to point, the plate can have variable thickness and may be actuated by a large variety of types of loads.

1. INTRODUCTION

In the analysis of plate structures lying on elastic soil two main methods have been used. One considers the plate as a rigid structure when compared with the soil. The other assumes that the plate is discretized in a net of finite differences, the soil being represented by springs with Winkler's coeficients [7].

In many cases the deformability of the plate must be taken into account since it changes the stress distribution. On the other hand the finite differences method has difficulties in dealing with plates with irregular geometry.

In this work we present a model for the analysis of plate structures resting on elastic soil formulated by the finite elements method and based in the Mindlin's theory. In this case the deformability of the plate is taken into account and no difficulties arise with irregular geometry.

2. NUMERICAL MODEL

2.1 Displacements

In the Mindlin's theory [1] the displacement $\underline{U} = \{u, v, w\}^T$ are expressed as function of the displacement of the middle surface $\overline{\underline{U}} = \{\overline{u}, \overline{v}, \overline{w}\}^T$ and of the rotations θ_x and θ_y of the normals to the middle surface in the planes YZ e ZX, respectively, according to the following relations (Fig. 1),

$$u(x,y,z) = z\,\theta_y(x,y) \tag{1}$$

$$v(x,y,z) = -z\,\theta_x(x,y) \tag{2}$$

$$w(x,y,z) = \overline{w}(x,y) \tag{3}$$

Fig. 1 — Displacements

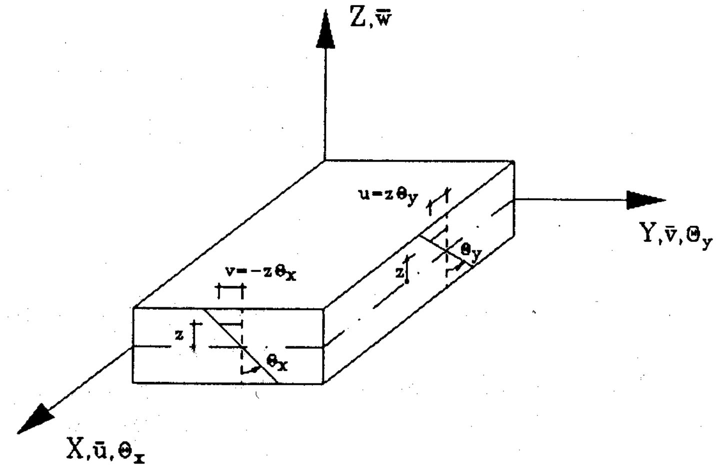

2.2 Deformations

Considering small displacement and that the u and v derivatives in order to x, y, z are also small and taking into account that w is independent of z, the strain vector will be given by the following relations:

$$\underline{\varepsilon} = \left\{ \begin{array}{c} \varepsilon_x \\ \varepsilon_y \\ \gamma_{xy} \\ \cdots \\ \gamma_{xz} \\ \gamma_{yz} \end{array} \right\} = \left\{ \begin{array}{l} \partial u/\partial x \\ \partial v/\partial y \\ \partial u/\partial y + \partial v/\partial x \\ \cdots\cdots\cdots\cdots\cdots \\ \partial u/\partial z + \partial w/\partial x \\ \partial v/\partial z + \partial w/\partial y \end{array} \right\} = \left\{ \begin{array}{c} z.\overline{\underline{\varepsilon}}^f \\ \\ \cdots \\ \\ \overline{\underline{\varepsilon}}^c \end{array} \right\} \tag{4}$$

where,

$$\overline{\underline{\varepsilon}}^f = \left\{ \begin{array}{l} \partial\theta_y/\partial x \\ -\partial\theta_x/\partial y \\ \partial\theta_y/\partial y - \partial\theta_x/\partial x \end{array} \right\} \; ; \; \overline{\underline{\varepsilon}}^c = \left\{ \begin{array}{c} \theta_y + \partial\overline{w}/\partial x \\ \\ -\theta_x + \partial\overline{w}/\partial y \end{array} \right\} \tag{5}$$

give the strains due to bending and shear, respectively. The vector of the generalized strains will take the form

$$\overline{\underline{\varepsilon}} = \left\{ \overline{\underline{\varepsilon}}^f, \overline{\underline{\varepsilon}}^c \right\}^T \tag{6}$$

2.3 Stress and forces

To the vector of strains refered in (4) corresponds the vector of Piolla-Kirchhoff stress,

$$\underline{\sigma} = \{\sigma_x, \sigma_y, \tau_{xy}, \tau_{xz}, \tau_{yz}\}^T \tag{7}$$

The generalized forces are obtained from (7) and are written as

$$\overline{\underline{\sigma}} = \left\{ \overline{\underline{\sigma}}^f, \overline{\underline{\sigma}}^c \right\}^T \tag{8}$$

where,

$$\overline{\underline{\sigma}}^f = \{M_{xx}, M_{yx}, M_{xy}\}^T = \left\{ \int_{-h/2}^{h/2} (\sigma_x, \sigma_y, \tau_{xy}) \cdot z \cdot dz \right\}^T \tag{9}$$

$$\overline{\underline{\sigma}}^c = \{Q_{xz}, Q_{yz}\}^T = \left\{ \int_{-h/2}^{h/2} (\tau_{xz}, \tau_{yz}) dz \right\}^T \tag{10}$$

which represent the bending and shear forces, respectively, h being the thickness of the element.

2.4 Constitutive relations

For an homogeneous and isotropic elastic material, with null stress on the z direction, the vector (8) is related to the vector of strains (6) by the expression:

$$\left\{ \begin{matrix} \underline{\overline{\sigma}}^f \\ \underline{\overline{\sigma}}^c \end{matrix} \right\} = \begin{bmatrix} [D^f] & [0] \\ [0] & [D^c] \end{bmatrix} \left\{ \begin{matrix} \underline{\overline{\varepsilon}}^f \\ \underline{\overline{\varepsilon}}^c \end{matrix} \right\} \tag{11}$$

where,

$$\left[D^f\right] = \frac{E \cdot h^3}{12(1-\nu^2)} \begin{bmatrix} 1 & \nu & 0 \\ \nu & 1 & 0 \\ 0 & 0 & \frac{1-\nu}{2} \end{bmatrix} \quad ; \quad [D^c] = G \cdot h \cdot k \begin{bmatrix} 1 & 0 \\ 0 & 1 \end{bmatrix} \tag{12}$$

are respectively the bending elasticity matrix and the shear elasticity matrix. The variables E, ν, G and k are the Young's modulus, the Poisson's ratio, the shear modulus and a corrective factor [2] to take into account the assumption of constant strain in the thickness of the element, formulated in the theory of Mindlin. For rectangular sections of isotropic materials k assumes the value of 5/6.

2.5 Strain matrices

The plate structures analysed by the model may be discretized in isoparametric elements of 8 nodes of the Serendipity type and of four and nine nods of the Lagrange [3–6]. Therefore, the generalized displacements at a internal point of a finite element will be obtained from the generalized displacements of its nodal points,

$$\underline{\overline{U}} = \sum_{i=1}^{n} [N_i \, I_3] \, \underline{\overline{U}}_i \tag{13}$$

where N_i is a shape function associated to the node i, $\underline{\overline{U}} = \{\overline{w}, \theta_x, \theta_y\}^T$ is the vector of the displacements of node i, I_3 is the unit matrix (3×3). Summation is extended to the number of nodal points of the element. Putting (13) into (4) the vector of strains (6) at any internal point of the element is writen in function of the nodal displacements,

$$\left\{ \begin{matrix} \underline{\overline{\varepsilon}}^f \\ \underline{\overline{\varepsilon}}^c \end{matrix} \right\} = \sum_{i=1}^{n} \begin{bmatrix} [B^f] \\ [B^c] \end{bmatrix}_i \left\{ \begin{matrix} \overline{w} \\ \theta_x \\ \theta_y \end{matrix} \right\}_i = \sum_{i=1}^{n} [B]_i \, \underline{\overline{U}}_i \tag{14}$$

where

$$\left[B^f\right] = \begin{bmatrix} 0 & 0 & \partial N/\partial x \\ 0 & -\partial N/\partial y & 0 \\ 0 & -\partial N/\partial x & \partial N/\partial y \end{bmatrix} \quad ; \quad [B^c] = \begin{bmatrix} \partial N/\partial x & 0 & N \\ \partial N/\partial y & -N & 0 \end{bmatrix} \tag{15}$$

correspond, respectively, to the bending and shear strain matrices.

2.6 Stiffness matrix

The stiffness matrix of the plate structure seting in an elastic media will have the contribution of the stiffness matrix of the structure plus the stiffness matrix of the soil, which model are springs orthogonal to the middle plane of the plate. The Winkler coefficients are the elements of the soil stiffness matrix.

2.6.1 Stiffness matrix of the plate structure

Assuming a virtual strain vector $d\underline{\overline{\varepsilon}}$, the virtual internal work of the stress $\underline{\overline{\sigma}}$ will be

$$dW_l = \int_A d\underline{\overline{\varepsilon}}^T\,\underline{\overline{\sigma}}\,dA \tag{16}$$

Putting (6), (8), (11) and (14) into (16), one obtains

$$dW_l = d\underline{\overline{U}}^T \int_A \left(\left[B^T\right][D]\,[B]\right) dA\,\underline{\overline{U}}^T \tag{17}$$

According to the virtual work theorem this is equal to the work done by the external forces: $d\underline{\overline{U}}^T \cdot \underline{\overline{F}}_e$. From that equality we obtain the stiffness matrix,

$$[K] = \int_A [B]^T\,[D]\,[B]\,dA \tag{18}$$

The matricial element k_{ij} of this matrix is given by

$$k_{ij} = \int_A \begin{bmatrix} \left[B^f\right]_i^T \left[D^f\right] \left[B^f\right]_j \\ + \\ \left[B^c\right]_i^T \left[D^c\right] \left[B^c\right]_j \end{bmatrix} dA \tag{19}$$

$i, j = 1, 2, ..., n$ (number of nodes of the element)

2.6.2 Stiffness matrix of the soil

Given the Winkler coefficients associated with the nodes of the structural element, the Winkler coefficient at any internal point of the element is given, in a isoparametric formulation, by

$$C_w(\xi,\eta) = \sum_{i=1}^{n} (C_w)_i\,N_i(\xi,\eta) \quad (20)$$

where $N_i(\xi,\eta)$ are the shape functions [3] refered in (13) and (ξ,η) the local coordinates of the element. The virtual vertical displacement at any internal point of the element is given through the virtual vertical displacement of the nodes of the element,

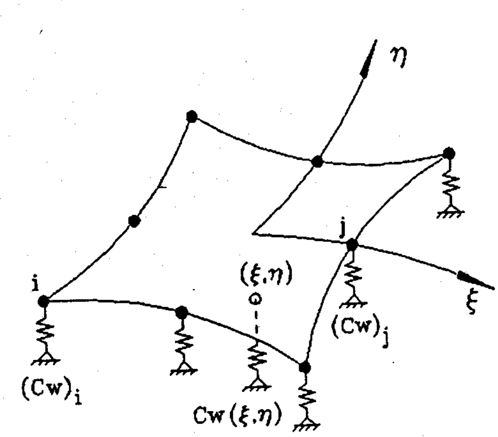

Fig. 2 — Soil model

$$d\overline{w}(\xi,\eta) = \sum_{i=1}^{n} d\overline{w}_i \, N_i(\xi\eta) \tag{21}$$

The internal virtual work done in the element is given by

$$dW_s = \int_A d\overline{w} \, C_W \, dA \tag{22}$$

Putting (20) and (21) into (22), using the virtual work theorem and applying the Gauss numerical integration, we obtain the stiffness coefficient corresponding to the generic nodes i and j of the element, associated with the contribution of the soil for the global stiffness of the soil/structure system,

$$(k_s)_{ij} = \sum_{p=1}^{Ng} \sum_{q=1}^{Ng} N_i(\xi_p,\eta_q) \cdot C_w(\xi_p,\eta_q) \cdot N_j(\xi_p,\eta_q) \cdot detJ \cdot w_p \cdot w_q \tag{23}$$

where $detJ$ is the determinant of the jacobian matrix [3] of the element which is related to the conversion of the global coordinates (x, y) to the local coordinates (ξ,η) of the element, Ng is the number of Gauss points of integration (two points for the elements of four nodes and three points for the element of eight and nine nodes) and w_p, w_q are the weights associated to the integration point (ξ_p, η_q) in the local coordinates system.

Notice that the soil stiffness, only affects the degree of freedom associated to the vertical displacement.

3. COMPUTATIONAL CODE

As already said our analysis is carried out in three phases: preprocessing, calculation and postprocessing. In this way it is possible to calculate structures of large dimensions in small computers, since for each programme only the necessary space in memory is reserved.

The main options in the computational code developped are the following:

1) Preprocessing programme:

   (1) creates files for finite elements grid generation; (2) generates the the finite elements grid; (3) renumbers the grid nodes; (4) creates data files. (2), (3) and (4) have graphical facilities.

2) Calculation programme:

   This program allows the calculation of displacement and reactions for each loading case.

3) Postprocessing programme:

   The options associated to this programme allow the graphical or numerical printing of results for each case of loading.

   The following are the options of this programme:

   (1) Data, (2) Nodal equivalent forces; (3) Displacements; (4) Coloring of the displacements; (5) Printing of the deflected structure; (6) Reactions; (7) Calculation and postprocessing of internal forces; (8) Coloring of the internal forces, (9) Internal forces diagrams; (10) Graphics of displacements and internal forces; (11) Pressures on the soil.

4. APPLICATIONS

Most of the results presented in the bibliography related to plate structures resting in elastic media, have been obtained by finite differences [7]. Therefore, in the following we compare the results obtained with our model with those obtained by finite differences, refered by other authors [7].

4.1 Rectangular footing

In Fig. 3 a rectangular footing resting on elastic media is presented (with a finite differences grid [7]). It has a vertical load at its center.

The data is the following:

$E_c = 22\,408\,730\ kN/m^2$ **(Young's modulus for the concrete of the plate)**

$C_w = 23536\ kN/m^3$ **(Winkler's coefficient for the soil)**

$\gamma_c = 23.56\ kN/m^3$ **(Specific weight of the concrete)**

In Fig. 4 we represent the network of finite elements, together with the principal moments in the footing.

In table 1 we present some of the results obtained with our model compared with those of reference [7].

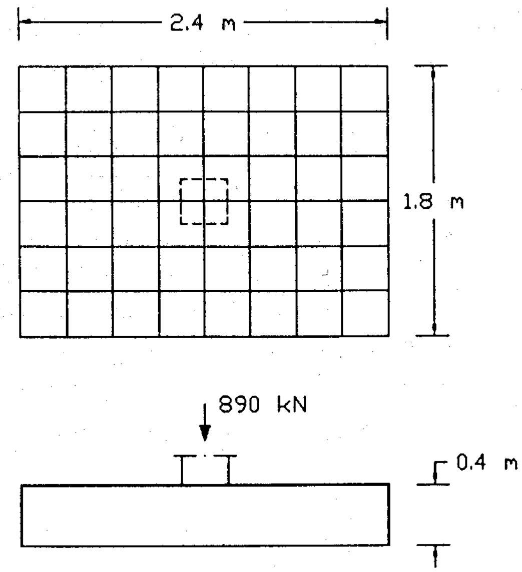

Fig. 3 — Rectangular footing resting on elastic media.

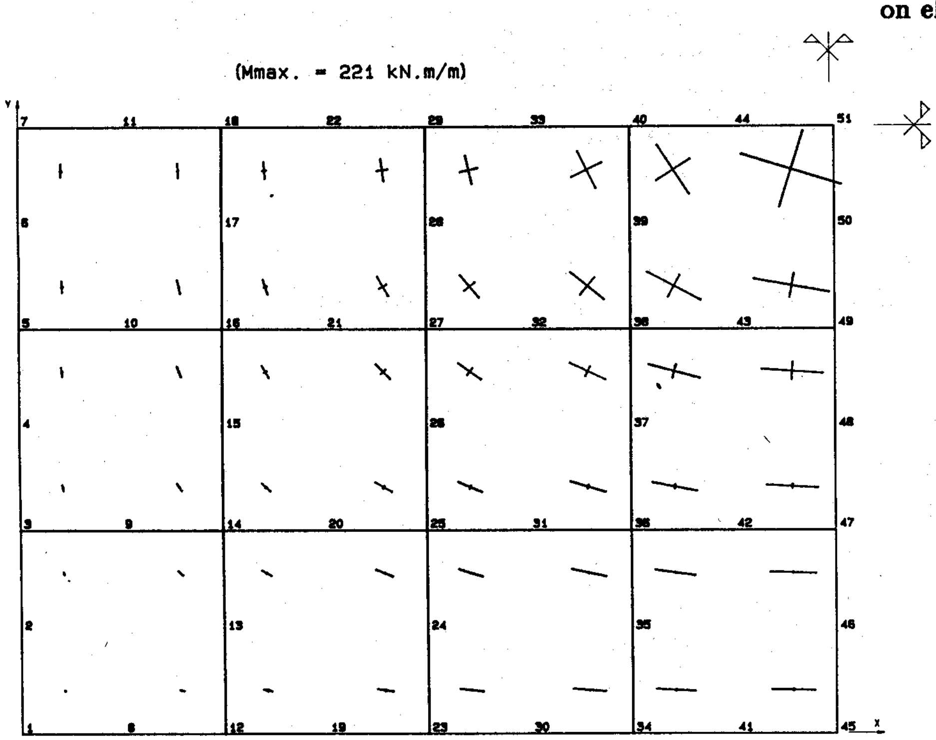

Fig. 4 — Principal moments

Node	Displacements ×100 (m)		Moments ($kN.m/m$)				Pressures (kN/m^2)	
			M_{xx}		M_{yx}			
	P. model	Ref. [7]	P. model(1)	Ref. [7]	P. model(1)	Ref. [7]	P. model	Ref. [7]
12	0.85781	0.89973	11.171	16.249	0	0	201.893	211.761
25	0.87472	0.91698	39.648	39.358	10.903	11.219	205.875	215.819
38	0.89196	0.93337	87.876	87.560	48.790	46.908	209.931	219.677
51	0.91539	0.94529	221.914	247.583	178.942	202.551	215.447	222.484

(1) Values extrapolated from the Gauss points to the node points with quadratic functions.

Table 1

4.2 Raft foundation

In Fig. 5 we present the grid of finite elements (8 nodes) for the raft foundation given in ref. [7]. The data is

$E_c = 22408776\, kN/m^2$

$\mu = 0.15$

$C_w = 5655.2\, kN/m^3$

$h = 1.168\, m$

Node	$F_z(kN)$	Node	$F_z(kN)$
1	-198.9	121	-763.6
3	-99.4	123	-381.0
7	-405.3	127	-1144.7
11	-116.7	131	-302.6
13	-233.4	133	-606.4
21	-73.7	141	-245.0
23	-36.8	143	-122.5
27	-150.1	147	-367.5
31	-43.2	151	-97.3
33	-86.5	153	-194.5
61	-245.0	181	-73.7
63	-122.5	183	-36.8
67	-367.5	191	-43.2
71	-97.3	193	-86.5
73	-194.5	201	-198.9
81	-763.6	203	-99.4
83	-381.0	207	-729.5
87	-1144.7	211	-116.7
91	-302.6	213	-233.4
93	-606.4		

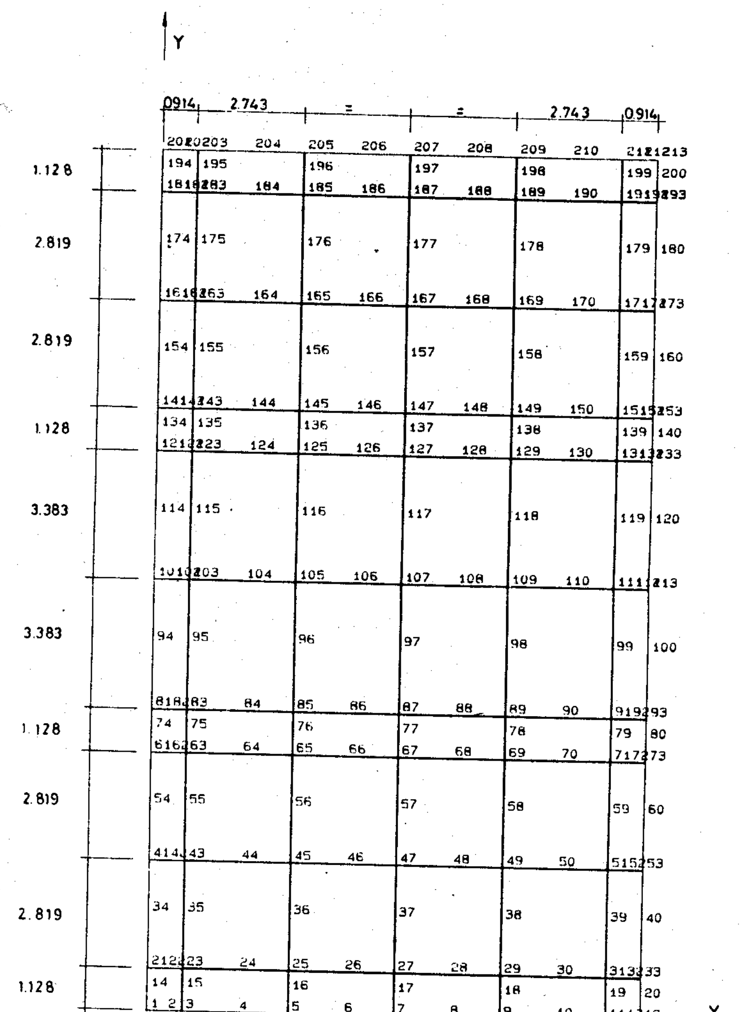

Fig. 5 — Grid of finite elements for the raft foundation.

We presents the results obtained from reference [7] (pp. 214–221) for the line,sectins A_1 and A_2 represented in fig 7:

Line section A_1 (m 0,914 = = = = = = = = = = = = =) → X

M_{xz} x (-1): 0,0 79,3 150,2 201,4 227,5 229,8 217,4 204,3 210,1 217,9 211,9 184,7 135,7 70,8 0,0

M_{yz} x (-1): 223,3 178,0 151,4 133,5 125,7 126,9 134,0 138,6 133,1 126,2 124,0 130,0 145,2 168,5 208,0
(kN.m/m)

Line section A_2 (m 0,914 = = = = = = = = = = = = =) → X

M_{xz} x (-1): 0,0 82,0 223,3 283,8 301,2 278,8 198,3 24,0 188,2 260,3 275,7 233,5 198,3 76,3 0,0

M_{yz} x (-1): 523,1 356,6 212,2 135,2 106,0 115,9 165,6 254,6 158,0 99,0 78,4 92,5 146,8 126,0 380,9
(kN.m/m)

In Fig. 6 the moments M_{xz} and M_{yz} (options of the programme) are plotted for sections S_1 and S_2 which contains the Gauss points nearer to the sections A_1 and A_2 of Fig. 7.

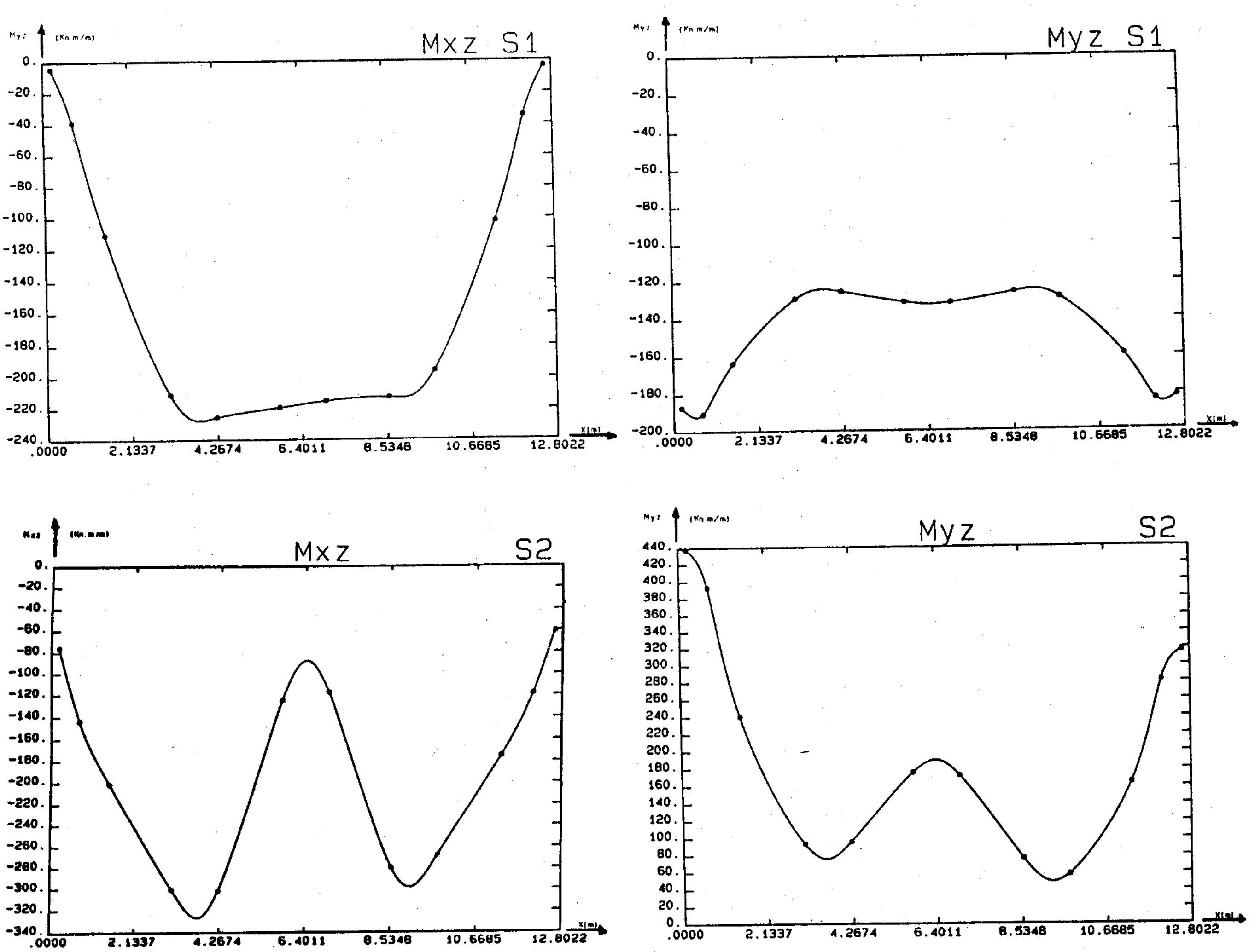

Fig. 6 — Graphics of the moments for sections S_1 and S_2.

In Fig 7 we present the principal moments. The coloring of the moments M_{xz} and M_{yz} developped in the plate and the soil pressures are given in Fig. 8. These results are some of the graphical options of our computational code.

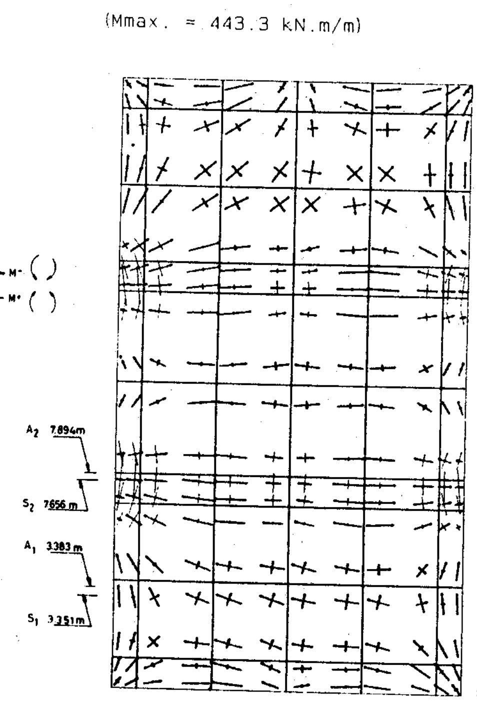

Fig. 7 – Principal moments.

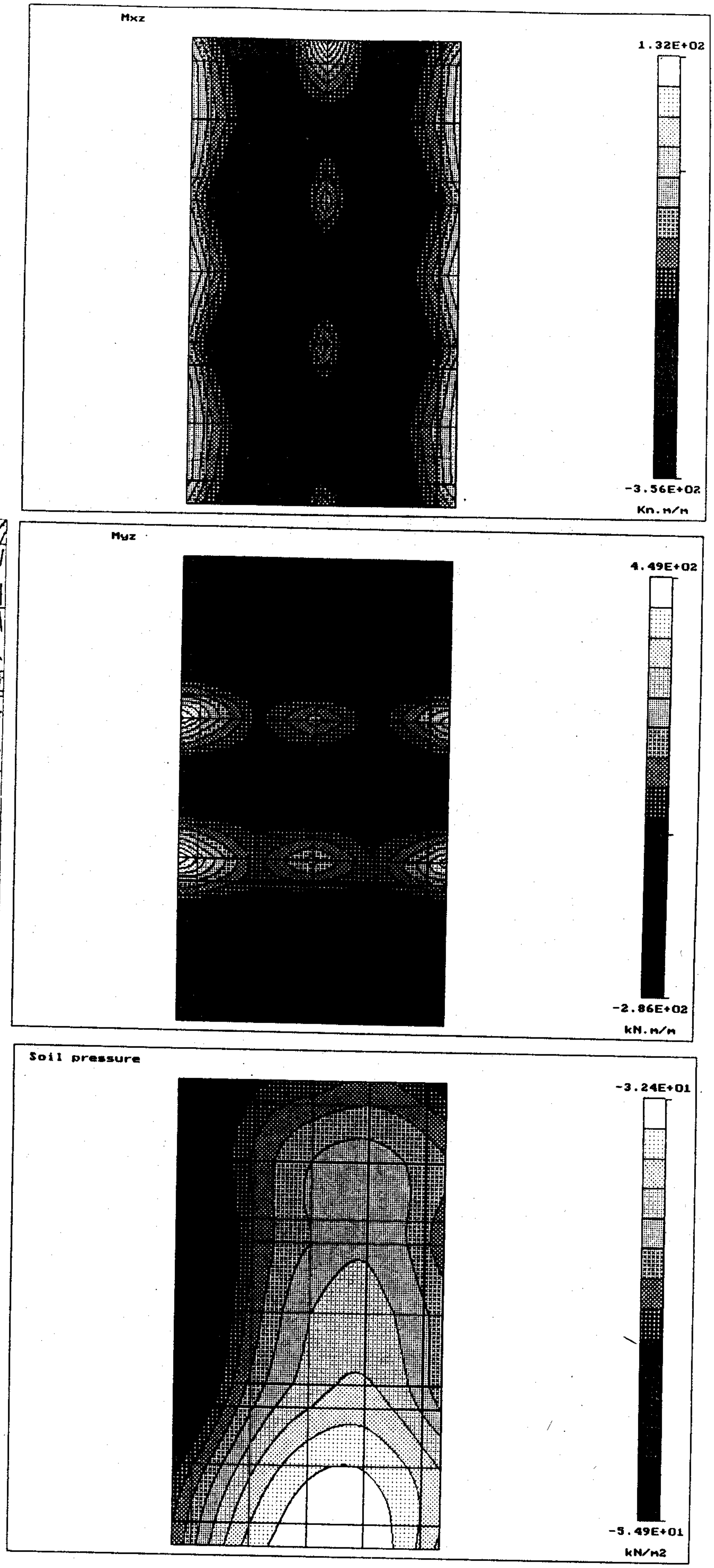

Fig. 8 – Coloring of the moments and soil pressures.

5. CONCLUSIONS

The modeling of the soil by springs with a linear behaviour and considering the plate-soil interaction, lead to a moment distribution quite different from that obtained by the simplified method of assuming an infinite stiffness for the plate in relation to the stiffness of the soil.

The graphical options of the computational code greatly contribute to the easy interpretation and analysis of the data and results.

6. BIBLIOGRAPHY

[1] R.D. MINDLIN, "Influence of rotary inertia and shear on flexural motions of isotropic, elastic plates", Journal of Appl., Vol. 18, No 1, Trans. ASME, vol. 73, 1951 pp. 31–38.

[2] J.A.O. BARROS, "Modelos de análise de estruturas laminares e de compósitos laminados", Tese de Mestrado, FEUP, Porto, 1989.

[3] O.C. ZIENKIEWICZ, "The finite element", third edition, McGraw-Hill, 1988.

[4] E. HINTON, D.R.J., "Finite element programming", Pineridge Press Ltd., 1980.

[5] D.R.J. OWEN, E. HINTON, "Finite elements in plasticity: theory and pratice", Pineridge Press Ltd, 1980.

[6] E. HINTON, D.R.J. OWEN, "Finite element software for plates and shells", Pineridge Press Ltd., 1981.

[7] J.E. BOWLES, "Analytical and computer methods in foundation engineering", McGraw-Hill, 1974.

[8] J.A.O. BARROS e J.A. FIGUEIRAS, "Análise de estruturas laminares utilizando elementos de casca planos com pré e pós processamento gráfico", FEUP, Porto, Dezembro de 1988.